Environmental Science & Technology

Article

pubs.acs.org/est

Uptake of Epoxydiol Isomers Accounts for Half of the Particle-Phase Material Produced from Isoprene Photooxidation via the HO_2 Pathway

Yingjun Liu,[||,†] Mikinori Kuwata,[||,†,⊥] Benjamin F. Strick,[‡] Franz M. Geiger,[‡] Regan J. Thomson,[‡] Karena A. McKinney,*[,†] and Scot T. Martin*[,†,§]

[†]School of Engineering and Applied Sciences, Harvard University, Cambridge, Massachusetts 02138, United States

[‡]Department of Chemistry, Northwestern University, Evanston, Illinois 60208, United States

[§]Department of Earth and Planetary Sciences, Harvard University, Cambridge, Massachusetts 02138, United States

Supporting Information

ABSTRACT: The oxidation of isoprene is a globally significant source of secondary organic material (SOM) of atmospheric particles. The relative importance of different parallel pathways, however, remains inadequately understood and quantified. SOM production from isoprene photooxidation was studied under hydroperoxyl-dominant conditions for <5% relative humidity and at 20 °C in the presence of highly acidic to completely neutralized sulfate particles. Isoprene photooxidation was separated from SOM production by using two continuously mixed flow reactors connected in series and operated at steady state. Two online mass spectrometers separately sampled the gas and particle phases in the reactor outflow. The loss of specific gas-phase species as contributors to the production of SOM was thereby quantified. The produced SOM mass concentration was directly proportional to the loss of isoprene epoxydiol (IEPOX) isomers from the gas phase. IEPOX isomers lost from the gas phase accounted for (46 ± 11)% of the produced SOM mass concentration. The IEPOX isomers comprised (59 ± 21)% (molecular count) of the loss of monitored gas-phase species. The implication is that for the investigated reaction conditions the SOM production pathways tied to IEPOX isomers accounted for half of the SOM mass concentration.

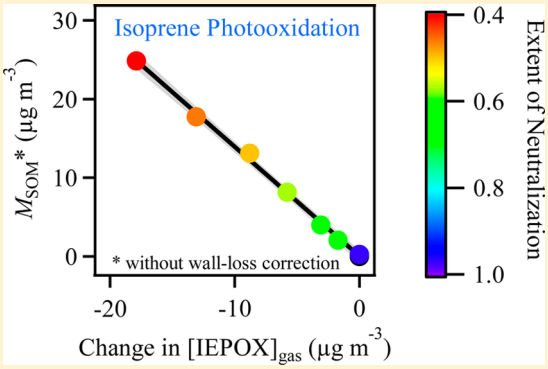

INTRODUCTION

Atmospheric particles are linked to adverse human health effects,[1] visibility impairment,[2] and anthropogenic changes to Earth's energy balance.[3] Secondary organic material (SOM) accounts for a large and sometimes dominant fraction of the mass concentration of submicron atmospheric particles.[4,5] SOM is produced as a result of the oxidation of volatile organic compounds (VOCs).[5] There are multiple parallel production pathways, including gas- and condensed-phase processes.[6] Because of the complexity of the processes involved, a quantitative and predictive understanding of SOM production is a major challenge in atmospheric chemistry research.[5]

The reaction pathways of a single species, namely isoprene, are estimated to contribute at least 25−50% of the annual global average of SOM production.[7−10] Predominantly emitted by vegetation, isoprene is the single largest source of nonmethane VOCs to the atmosphere.[11] Under atmospheric conditions, oxidation of isoprene is initiated primarily by hydroxyl radicals (OH) followed by the addition of molecular oxygen (O_2) to produce a population of reactive peroxyl radical intermediates (RO_2).[12] The subsequent fate of these RO_2 radicals is to follow multiple reaction pathways, resulting in many different products in the gas and particle phases. Molecular tracers of isoprene oxidation, such as 2-methylbutanetetrols, C_5-alkene triols, organosulfates, and oligomeric species, have been identified in SOM sampled at locations worldwide.[13−18]

A quantitative understanding of the multiple reaction pathways that contribute to SOM production from isoprene photooxidation is a critical step in the formulation of accurate models of atmospheric particle mass concentrations.[19] Recent laboratory and ambient findings demonstrate that isoprene epoxydiol (IEPOX) isomers, which are produced by the further reactions of the population of RO_2 intermediates with hydroperoxyl (HO_2) and then hydroxyl radicals,[20] serve as at least one set of important products to produce SOM,[21−26] especially by reactive uptake to acidic sulfate particles.[21−23,26] The IEPOX isomers include *trans*-β-IEPOX, *cis*-β-IEPOX, δ1-IEPOX, and δ4-IEPOX (Supporting Information (SI) Figure S1), of which the β isomers dominate (>97%) for typical reaction conditions.[27] Known IEPOX-derived particle-phase

Received: July 15, 2014
Revised: October 16, 2014
Accepted: November 6, 2014
Published: November 6, 2014

molecules account for at least 20% of the mass of isoprene-derived SOM in the laboratory.[21] The result is a lower limit given that not all IEPOX-derived products are known (i.e., an incomplete set of molecular tracers).

The quantitative determination of the relative contribution of the IEPOX pathway to SOM production from isoprene photooxidation is the goal of the present study. Although the IEPOX pathway has been suggested as an important pathway for SOM production from isoprene photooxdation, direct quantitative evidence nevertheless remains lacking, and other reaction pathways might also be quantitatively important, such as oligomer production via hydroperoxide pathways.[15,28]

EXPERIMENTAL SECTION

In overview, two continuously mixed flow reactors were connected in series and operated at steady state as an experimental strategy to separate isoprene photooxidation from SOM production (Figure 1). In Reactor 1 (viz. the Harvard Environmental Chamber; HEC), gas-phase isoprene oxidation products were continuously produced. In Reactor 2, the outflow of the HEC was mixed with a flow of sulfate particles. As a result, the signal change of a gas-phase species in Reactor 2 was due to the molecular uptake or release of the species from the sulfate particles.

Reaction Conditions. Reactor 1 (i.e., the HEC) was operated as a continuously mixed flow reactor at steady state. Photolysis of H_2O_2 by ultraviolet light produced OH radicals, initiating isoprene oxidation.[29] The inflow and steady-state isoprene concentrations were 120 ± 5 ppb and 36 ± 1 ppb, respectively. The mean residence time was 3.7 ± 0.3 hr. No new particle production was observed inside Reactor 1, as confirmed by a condensation particle counter (CPC; <0.5 particle cm^{-3}).

Photooxidation in Reactor 1 corresponded to reaction conditions such that the isoprene-derived RO_2 radicals reacted dominantly with HO_2,[29] which is the main reaction pathway in unpolluted regions having sufficiently low NO_x concentrations.[30−32] Previous experiments and model simulations confirmed that the fate of isoprene-derived RO_2 radicals was dominated by the reaction with HO_2 for the experimental conditions employed in this study.[29]

In Reactor 2, sulfate particles of variable acidity were employed to promote multiphase reactions representative of atmospheric processes.[21,33,34] Acidic sulfate particles were produced by exposing ammonium sulfate particles to sulfuric acid vapor. Size-selected crystalline ammonium sulfate particles were generated by using an atomizer, a diffusion dryer, and a differential mobility analyzer (DMA) in series (cf. SI as well as ref 35). The central mobility diameters of particles carrying a single or double positive charge were 50 ± 2 and 72 ± 3 nm, respectively. Sulfuric acid vapor was produced by heating a concentrated solution (96% w/w) of sulfuric acid to 20 to 60 °C.[36] The mass of depositing vapor on the ammonium sulfate particles was regulated by the heater temperature, ultimately determining the extent X of neutralization of the mixed particles. The quantity X is defined as $n(NH_4^+)/(2n(SO_4^{2-}))$ for ion mole concentration n(ion) (mol m^{-3}) and ranges from 0 for sulfuric acid to 1 for ammonium sulfate. New particle production from sulfuric acid vapor was not observed for the temperature range employed.

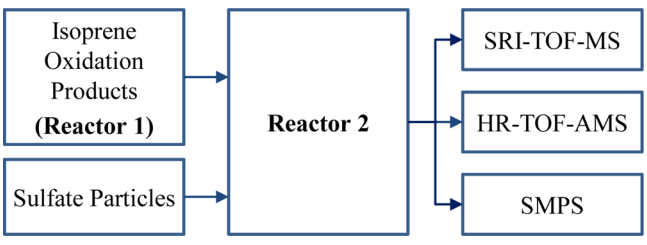

Figure 1. Schematic of experimental setup. Abbreviations are defined in the main text.

The flows of gas-phase oxidation products from Reactor 1 and of sulfate particles from the generator were mixed together in Reactor 2 (72 L, made of glass). Reactor 2 served as the second continuously mixed flow reactor, also operated at steady state. The temperature, relative humidity, and flow were 20 ± 1 °C, < 5%, and 0.87 Lpm, respectively. The reactor was covered in aluminum foil to avoid irradiation by laboratory lighting. Particle injection was switched by adjusting the DMA voltage rather than altering flows. Variation of the inflow rates, as indicated by the isoprene signal, was below 5%, and changes in the dilution ratio because of flow variability were corrected using the measured isoprene signal. For photooxidation products measurable by the chemical ionization mass spectrometry employed in the present study (vide infra), no significant wall loss was observed in Reactor 2 at steady state in the absence of sulfate particles, as demonstrated by a comparison of the mass spectrum of air sampled directly from Reactor 1 with that sampled from Reactor 2 (SI Figure S2).

For selected experiments, instead of using photooxidation products from Reactor 1, a gas flow containing *trans-β*-IEPOX was injected into Reactor 2. For volatilization, a drop of *trans-β*-IEPOX was placed inside of a Teflon T-fitting. The fitting was flushed by purified air, thereby producing a gas stream containing a trace amount of *trans-β*-IEPOX. These experiments provided reference spectra of IEPOX-derived SOM, as a comparison point for the SOM spectra collected in the main experiments. The IEPOX signal in the gas-phase flow into Reactor 2 was, however, not stable enough to allow for any quantitative analysis.

Gas-Phase and Particle-Phase Measurements. Gas- and particle-phase mass spectra of the outflow from Reactor 2 were recorded by a selective-reagent-ionization time-of-flight mass spectrometer (SRI-TOF-MS; NO^+ reagent; Ionicon Analytik GmbH)[37,38] and a high-resolution time-of-flight aerosol mass spectrometer (HR-TOF-AMS; electron-impact ionization; Aerodyne Research Inc.),[39] respectively. Soft chemical ionization by NO^+ (9.26 eV) of the gas-phase sample typically resulted in one or a few product ions, and attribution of ions to specific molecules was possible.[40] By comparison, electron-impact ionization (70 eV) of the particle-phase material decomposed molecules into many small fragment ions. Even so, the overall spectral pattern of fragment ions could be related to the original chemical composition.[39]

The SRI-NO^+-TOF-MS settings and data analysis procedures were published earlier.[29] Briefly, peaks over the whole spectrum were fit, and their corresponding ion compositions were determined. Intensities of ion signals for isoprene and methacrolein were calibrated daily, and the observations indicated a stable instrument response during the experimental period. The ion transmission curve of the SRI-TOF-MS was measured using H_3O^+ as the reagent ion.[41] Ion transmission was taken into account when comparing the intensities of any

Table 1. Summary of Experimental Conditions and Observations[a]

	HR-TOF-MS			SRI-NO$^+$-TOF-MS		
experiment	X	$M_{sulfate}$ (μg m^{-3})	M_{SOM}[b] (μg m^{-3})	$\Delta_{C_5H_6O^+}/\Sigma\Delta$[c] (%)	$[IEPOX]_{gas}$[d] (μg m^{-3})	M_{IEPOX}/M_{SOM}[e] (%)
1	NA[f]	<MDL[g]	<MDL	NA	38.5 ± 0.5 (7.7)	NA
2	0.97 ± 0.07[h]	0.8 ± 0.1	<MDL	<MDL	38.5 ± 0.4 (7.7)	<MDL
3	0.69 ± 0.04[i]	1.2 ± 0.1	2.1 ± 0.1 (3 ± 1)	72 ± 13 (19)	36.8 ± 0.5 (7.4)	54 ± 26
4	0.64 ± 0.04	1.3 ± 0.1	4.0 ± 0.1 (7 ± 1)	60 ± 8 (16)	35.4 ± 0.5 (7.1)	49 ± 17
5	0.57 ± 0.03	1.8 ± 0.1	8.1 ± 0.2 (14 ± 3)	63 ± 5 (14)	32.7 ± 0.3 (6.5)	45 ± 12
6	0.50 ± 0.03	2.1 ± 0.1	13.1 ± 0.3 (22 ± 4)	55 ± 3 (13)	29.7 ± 0.2 (5.9)	43 ± 11
7	0.46 ± 0.03	2.8 ± 0.1	17.8 ± 0.4 (30 ± 6)	47 ± 3 (13)	25.4 ± 0.3 (5.1)	47 ± 11
8	0.39 ± 0.02	3.5 ± 0.1	24.9 ± 0.3 (42 ± 8)	56 ± 3 (13)	20.6 ± 0.5 (4.1)	46 ± 11
Summary				**59 ± 17 (21)**[j]		**46 ± 11**[k]

[a]Experiments were conducted for <5% relative humidity and at 20 °C. [b]M_{SOM} is the measured particle organic mass concentration. The number in the parentheses is the wall-loss corrected particle organic mass concentration. [c]$\Delta_{C_5H_6O^+}/\sum\Delta$ is the contribution of the decrease of $C_5H_6O^+$ signal to the total of signal decreases across the full spectrum. It is used as an estimate of the contribution of IEPOX isomers to the total loss of organic species in the gas phase (molecular counts). There is an increase in the uncertainty for the latter (shown in parentheses) to take into account of the differences in the NO$^+$ reaction rate coefficients with different compounds. [d]$[IEPOX]_{gas}$ is the steady-state gas-phase concentration of IEPOX isomers in Reactor 2. The presented uncertainty reflects twice the standard deviation of IEPOX signal in each experiment to facilitate interexperimental comparison. The number in the parentheses is the uncertainty considering additional systematic error associated with the IEPOX sensitivity applied to the whole set of experiments. [e]M_{IEPOX}/M_{SOM} is the contribution of IEPOX isomers to the production of isoprene SOM. M_{IEPOX} was the SOM produced from IEPOX pathways, estimated using the decrease of gas-phase mass concentration of IEPOX isomers (cf. Main Text). [f]Not Applicable (NA). [g]Method detection limit (MDL). [h]Sulfate particles are solid. [i]Sulfate particles are at least partially aqueous.[53,54] [j]An estimate for the complete set of experiments by bootstrapping the results of individual experiments (cf. SI). [k]An estimate for the complete set of experiments by fitting M_{SOM} vs $[IEPOX]_{gas}$ (Figure 5a).

two ions and when calculating the total signal intensity across the full spectrum. A 2.0-μm pore size Teflon filter was used to remove particles upstream of the SRI-NO$^+$-TOF-MS, thereby avoiding complicating factors such as clogging of the inlet or wall deposition. Control studies suggested a negligible effect of the particle filter on the measured gas-phase signals of the outflow of Reactor 2 (cf. SI).

The particle-phase mass spectra measured by the HR-TOF-AMS were used to quantify the mass concentration M_{SOM} of the produced SOM and to characterize the SOM composition. Ammonium nitrate was used for calibration of the ionization efficiency, which is the major factor affecting quantification of mass concentration. Both mass concentration and unit resolution mass spectra were analyzed using the data analysis software package Sequential Igor Data Retrieval (SQUIRREL ver. 1.51H). High resolution data analysis was performed by Peak Integration by Key Analysis (PIKA ver. 1.10H).

The outflow of Reactor 2 was also sampled by a scanning mobility particle sizer (SMPS; TSI Inc.) to measure the number-diameter distribution of the particle population. The SMPS consisted of a DMA (TSI 3081) and a CPC (TSI 3776). The DMA voltage was scanned from 32 to 6358 V, corresponding to a diameter range of 25.5−487 nm for a sheath flow of 3.0 Lpm and a sample flow of 0.3 Lpm. The scanning time of the DMA was 100 s. The overall time resolution of the measurement was 120 s.

Cold Trapping and Re-Evaporation of Oxidation Products. The relative volatilities of gas-phase oxidation products present in the outflow from Reactor 1 were examined by cold trapping and re-evaporation. The outflow from Reactor 1 passed through a 1-m Teflon PFA coil immersed in a liquid bath at −40 °C for 4 hr. After this collection period, the coil was purged using a flow of dry purified air while increasing the bath temperature at 5 °C hr^{-1}. The flow was sampled by the SRI-NO$^+$-TOF-MS. Molecules of progressively lower vapor pressures sequentially evaporated into the purified air, and the time series analysis of the mass spectra provided characterization of the products. SI Figure S3 shows the time series of the intensities of some selected ions. The main purpose of these experiments was to show cross-check consistency for the assignment of the $C_5H_6O^+$ ion as IEPOX compounds (vide infra).

Instrument Characterization and Calibration Using Synthesized IEPOX Compounds. Four IEPOX isomers were synthesized.[42] The purity of the IEPOX compounds was confirmed by nuclear magnetic resonance (NMR) spectroscopy (SI Figures S4−S7). Reference mass spectra were obtained by sampling a gas flow containing individual IEPOX isomers into the SRI-NO$^+$-TOF-MS (SI Figure S8).

In addition to the reference mass spectra, the sensitivity of the SRI-NO$^+$-TOF-MS to the *trans*- and *cis*-β-IEPOX isomers was determined, as follows. An aqueous solution (0.05−0.2 g L^{-1}) containing one IEPOX isomer was nebulized (Meinhard TR-30-A1). The nebulizer was fed (0.1−0.2 mL hr^{-1}) using a gastight syringe (Hamilton 1002LT) placed in a syringe pump (Chemyx Fusion 200). The gas flow into the nebulizer was 1 sLpm. The nebulizer outflow was further mixed with a purified air flow at 1 sLpm in a glass mixing flask (100 mL) to allow full evaporation of the nebulized droplets to take place. No liquid condensation was visible on the walls of the flask. After sufficient time, steady signals were observed by SRI-NO$^+$-TOF-MS (SI Figure S9), indicating that equilibrium with the walls was attained (all surfaces were glass or Teflon). The steady-state gas-phase IEPOX concentration in the outflow of the mixing flask (10−65 ppb) was calculated based on the solution concentration and the several dilution flows.

RESULTS AND DISCUSSION

The first three sections of the results and discussion are organized from the perspectives of the gas phase, the particle phase, and the link between the gas and particle phases, respectively, all aiming to assess the relative contribution of the IEPOX pathway to SOM production from isoprene photo-

oxidation. The final section considers the atmospheric implications.

A general overview of the experiments and observations is presented in Table 1. The extent X of neutralization listed in the second column corresponds to the sulfate particles injected into Reactor 2. Upon injection and mixing with the isoprene photooxidation products, secondary organic material was produced (M_{SOM}). Corresponding changes in the gas-phase composition are listed in the subsequent columns of Table 1. The rows of Table 1 correspond to a series of experiments that varied X stepwise from 0.97 ± 0.07 to 0.39 ± 0.02, associated with sulfate concentrations of 0.8 ± 0.1 to 3.5 ± 0.1 μg m^{-3}. The entries in Table 1 show that SOM production was insignificant for solid neutral particles (X = 0.97 ± 0.07) and increased for aqueous acidic particles from 2.1 ± 0.1 μg m^{-3} for X = 0.69 ± 0.04 to 24.9 ± 0.3 μg m^{-3} for X = 0.39 ± 0.02.[35] The accompanying changes in the gas-phase species (Table 1) reveal two results (vide infra): the IEPOX isomers comprised (59 ± 21)% (molecular count) of the loss of monitored gas-phase species, and the mass concentration of IEPOX isomers lost from the gas phase accounted for (46 ± 11)% of the produced SOM mass concentration.

Loss of Gas-Phase Species. Figure 2a shows two examples of high-resolution mass spectra collected by sampling of the gas-phase outflow from Reactor 2. The two spectra correspond to the absence and the presence of acidic particles (X = 0.39 ± 0.02) in Reactor 2. Many peak intensities did not change significantly following the injection of acidic particles, such as those for ions originating from unreacted isoprene ($C_5H_8^+$, m/z 68.0621), hydrogen peroxide ($H_2O_2{\cdot}NO^+$, m/z 64.0029), and some oxidation products (e.g., $C_3H_6NO_3^+$, m/z 104.034). By comparison, some other peak intensities, mostly those arising from C_4^+ and C_5^+ ions of isoprene oxidation products, such as $C_5H_6O^+$ (m/z 82.0413) and $C_5H_7O_2^+$ (m/z 99.0441), decreased following the injection of acidic particles. The change of −81 ncps in normalized signal intensity of the $C_5H_6O^+$ ion was eight times greater than the next largest change, which was −10 ncps for $C_5H_7O_2^+$. The unit ncps is the signal in counts per second (cps) normalized (n) to a NO^+-reagent-ion signal of 10^6 cps.

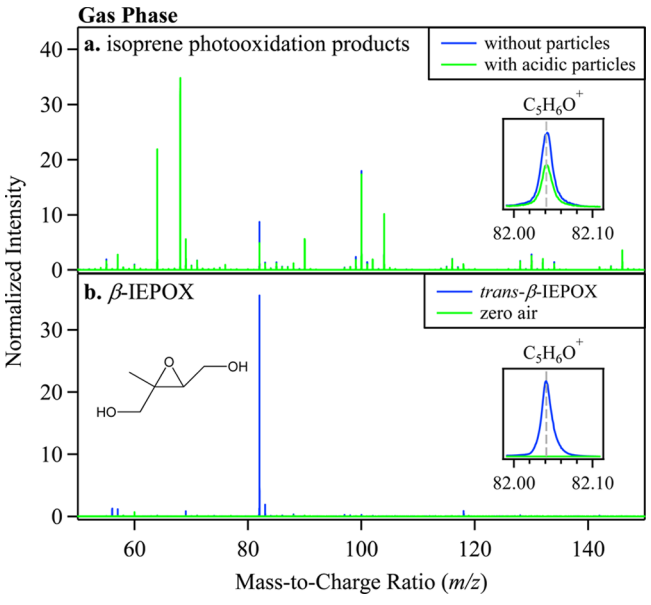

Figure 2. Mass spectra collected by SRI-NO^+-TOF-MS. (a) Isoprene photooxidation products of outflow of Reactor 2 in the presence (green) and absence (blue) of acidic particles (X = 0.4). (b) Reference conditions of *trans*-β-IEPOX (blue) and zero air (green). Inset shows an expansion near m/z 82, corresponding at m/z 82.0413 to $C_5H_6O^+$. Spectrum intensities are normalized to the signal intensity of the NO^+ reagent ion.

On the basis of characterization using authentic compounds, the $C_5H_6O^+$ ion is attributed to the ionization of β-IEPOX (i.e., *trans*-β-IEPOX + *cis*-β-IEPOX; $C_5H_{10}O_3$). Specifically, $C_5H_6O^+$ was the dominant product ion for authentic β-IEPOX isomers, as obtained using the NO^+ reagent ion (Figure 2b and SI Figure S8). The ion arose from charge transfer of NO^+ with β-IEPOX followed by dehydration (i.e., $((C_5H_{10}O_3)\text{-}2(H_2O))^+$). Although this ion also appeared as one fragment of the two δ-IEPOX isomers (SI Figure S8), ref 27 found that the δ isomers accounted for <3% of the IEPOX isomers produced from isoprene photooxidation.

Another data set, based on cold trapping and re-evaporation of the isoprene photooxidation products exiting Reactor 1, gives further support that the $C_5H_6O^+$ ion arose dominantly from IEPOX isomers, rather than other possible known oxidation products. Methyl furan (C_5H_6O) is an oxidation product of isoprene which also gives rise to $C_5H_6O^+$ upon reaction with NO^+. In control studies, methyl furan obtained as a pure compound was not trapped at the temperature employed (results not shown). For the outflow from Reactor 1, over 95% of the $C_5H_6O^+$ signal intensity was removed by the cold trap, implying that methyl furan was not a major contributor to this ion. The spectra recorded upon heating the trap (SI Figure S3) showed that $C_5H_6O^+$ arose dominantly from compounds having long retention times and hence low vapor pressures, as expected for IEPOX isomers (~0.3 Pa).[43] By comparison, many other trapped products, such as the isoprene-derived hydroperoxide precursors of the IEPOX isomers,[20] had shorter retention times, as expected for these higher-volatility compounds (~0.6 Pa).[43] Even so, the possibility remains that unknown reaction products might have vapor pressures similar to those of the IEPOX isomers and might also give rise to the $C_5H_6O^+$ ion.

The decreases in peak intensities observed by SRI-NO^+-TOF-MS upon mixing with sulfate particles were analyzed to estimate the contribution of IEPOX isomers to the total loss of gas-phase species. The decrease (ncps) at each ion peak was calculated. Decreases greater than three times the standard deviation of the noise at each signal were taken as significant. The sum (ncps) across all significant decreases was calculated. The combined decreases of the $C_4{}^{12}CH_6O^+$ and $C_4{}^{13}CH_6O^+$ signals (i.e., common $C_5H_6O^+$ isotopologues) accounted for (56 ± 3)% of the total for the experiment shown in Figure 2a and (59 ± 17)% across all experiments (Table 1). By comparison, the next largest contribution for the experiment shown in Figure 2a was (7 ± 3)% ($C_5H_7O_2^+$). Uncertainties are given to 2δ (95%) unless stated otherwise. Further information on uncertainty estimates is provided in the SI.

For the present study, the percent contributions in the decreases of peak intensities of the SRI-NO^+-TOF-MS spectrum are assumed as equivalent to the percent contributions in actual concentrations. This assumption is believed reasonable within the uncertainties because the ionization reactions of NO^+ with oxygenated organic compounds are usually collision limited.[40] The uncertainty estimate in the percent contributions for the concentrations takes into account possible differences in the NO^+ reaction rate constant among

dx.doi.org/10.1021/es5034298 | Environ. Sci. Technol. 2015, 49, 250−258

the different compounds (±50%) and hence is larger than that for the signal intensities (Table 1). For the estimate using the whole set of experiments, uncertainty increased from 17% for signal intensity to 21% for concentration. Further discussion is provided in the SI.

The finding is that IEPOX isomers accounted for (59 ± 21)% of the total gas-phase species concentrations (molecular count) removed on exposure to acidic sulfate particles. This finding implies that IEPOX likewise accounted for (59 ± 21)% of the SOM produced during isoprene photooxidation in the presence of acidic particles. This estimate is based on molecular count rather than mass. An estimate based on mass concentration is presented further below.

SOM Chemical Composition. The mass spectrum of SOM produced by the uptake of isoprene photooxidation products was compared to that obtained for SOM produced by the uptake of β-IEPOX, both in the presence of acidic particles. The unit mass resolution spectrum of isoprene-derived SOM had marker peaks at m/z 82 ($C_5H_6O^+$) and 101 ($C_5H_9O_2^+$) (Figure 3a). There were also peaks (m/z < 60) at m/z 27, 28, 29, 39, 41, 43, 44, 53, and 55. These characteristic peaks, described both by the m/z values as well as the intensities relative to one another, were similar to those present in the mass spectrum of β-IEPOX SOM, both as recorded in the current study (Figure 3b) as well as reported in the literature (Figure S10).[24,25] The fraction of m/z 82, which has been used as a marker ion in the interpretation of ambient data,[24,44−46] was (2.9 ± 0.1)% for SOM derived from chamber oxidation products and (3.6 ± 0.1)% for that derived from β-IEPOX. The similarity of the mass spectrum of isoprene-derived SOM to that of β-IEPOX SOM provides further support for the conclusion that IEPOX isomers were the dominant carbon contributors to SOM production during isoprene photooxidation, at least for the conditions of this study (i.e., HO_2-dominant reaction conditions in the presence of acidic particles at low relative humidity).

The mass spectrum of isoprene-derived SOM obtained from this study can be compared with results obtained for ambient particles in or nearby isoprene source regions. Available data sets include those from Borneo,[44] the central Amazon,[46] Atlanta,[24] and Ontario.[45] Positive-matrix factorization (PMF) of the mass spectra collected in these locations resolved in all four cases a statistical factor attributed at least in part to isoprene-derived SOM (cf. Figures 3c-3f). The factors have in common a characteristic peak at m/z 82, which was also present in the isoprene-derived SOM of the present study (Figure 3a). High-resolution analysis of these mass spectra shows that the $C_5H_6O^+$ ion was the dominant contributor to this peak.[44−46]

Figures 4a−d present correlation plots between the mass spectrum of isoprene-derived SOM and the PMF factors. For the Borneo data, there is close clustering along the 1:1 line, with an exception for m/z 44 (Figure 4a). Good correlation with the Amazon factor is also apparent except for m/z 44 and m/z 28 (Figure 4b). The differences at m/z 44 might arise from additional oxidation and photochemical processing during the particle atmospheric lifetime, that is, processes which were not

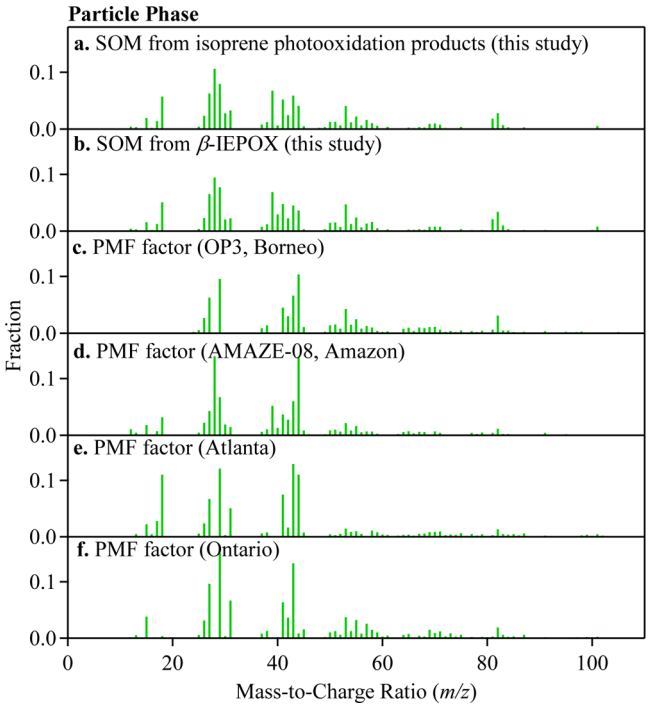

Figure 3. Mass spectra collected by HR-TOF-AMS of outflow of Reactor 2. (a) SOM produced by isoprene photooxidation products in the presence of acidic particles (X = 0.6). (b) SOM produced from *tran*-β-IEPOX in the presence of acidic particles (X = 0.6). (c) Isoprene-related PMF factor from Borneo (OP3).[44] (d) Isoprene-related PMF factor collected during the wet season of the central Amazon (AMAZE-08).[46] (e) Isoprene-related PMF factor from Atlanta.[24] (f) Isoprene-related PMF factor from Ontario.[45] There was no significant change in the fractional contributions of the major peaks in panels *a* and *b* with extent X of neutralization for the conducted experiments (results not shown).

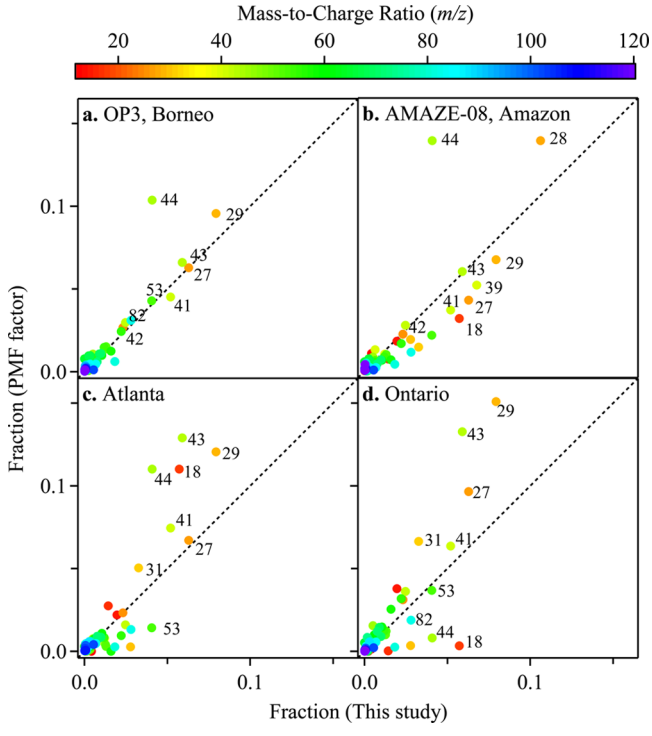

Figure 4. Correlation plot between the normalized mass spectrum of isoprene-derived SOM for this study (X = 0.6) and the isoprene-related PMF factors from ambient data sets obtained in (a) Borneo (OP3),[44] (b) the Amazon (AMAZE-08),[46] (c) Atlanta,[24] and (d) Ontario.[45] Correlation plots are based on unit-mass-resolution spectra.

dx.doi.org/10.1021/es5034298 | Environ. Sci. Technol. 2015, 49, 250−258

captured in the current laboratory study. Overall, there is positive but nevertheless weaker correlation with the factors from Atlanta (Figure 4c) and Ontario (Figure 4d).

One possible explanation for the different levels of correlation in the panels of Figure 4 is that the SOM of the present study corresponds to fresh production from isoprene photooxidation via the HO_2 pathway in the presence of acidic particles whereas the range of atmospheric conditions and processes is broader. These laboratory conditions might more closely resemble remote isoprene source regions like Borneo and Amazon than to regions having large urban influences like Atlanta and Ontario (i.e., more NO_x and more NH_3). The overall caveat must also be kept in mind that all four study locations were subject to complex local environmental and chemical factors not captured in the present laboratory study, such as differences in relative humidity (i.e., <5% in present study) as well as possible interactions with the multiple organic species in the atmosphere. A second caveat is that the presented results cannot rule out the possibility that other isoprene reaction pathways, as yet uninvestigated, might also give rise to a similar mass spectrum as IEPOX uptake under laboratory conditions and that these other SOM production processes might thereby also contribute to the observed PMF factors. These two caveats notwithstanding, however, the positive correlations of Figure 4 do substantially underpin that the PMF factors identified for atmospheric data sets can be associated at reasonable likelihood with reactive uptake under acidic conditions of isoprene oxidation products along the HO_2 pathway, in particular IEPOX isomers.

Uptake of IEPOX Isomers and Production of SOM. Figure 5a shows a scatter plot between the steady-state mass concentration $[IEPOX]_{gas}$ of IEPOX isomers in the gas phase and the mass concentration M_{SOM} of SOM in the outflow of Reactor 2. $[IEPOX]_{gas}$ was calculated from the intensities of the $C_5H_6O^+$ ion using a sensitivity for IEPOX isomers (4.5 ± 0.4 ncps μg^{-1} m^3) derived from the measured sensitivities of *cis*- and *trans*-β-IEPOX (cf. SI). The plot shows that the production of M_{SOM} correlated (R^2 = 0.99) with the loss of gas-phase IEPOX isomers across the range of investigated X. The correlation further confirms that the reactive uptake of IEPOX isomers, which were present in the suite of isoprene photooxidation products produced in Reactor 1, was a contributing process to SOM production.

The relative contribution of IEPOX isomers to SOM production, compared to other possible contributors, was estimated by comparing on a mass basis the gas-phase loss of IEPOX isomers to SOM production. The SOM production was based on the mass concentration measured by the HR-TOF-AMS and corrected for wall loss in Reactor 2. Of the sulfate particles injected, (41 ± 4)% were lost to the walls based on the particle number concentrations measured upstream and downstream of Reactor 2, implying a wall-loss correction factor for M_{SOM} of 1.7 ± 0.3. The assumption in this analysis is that the particles deposited to the walls were similar to those in the outflow (i.e, no further growth given a longer exposure time), as justified by additional experiments showing that diameter growth of the particle population in Reactor 2 ceased when the injection of sulfate particles was stopped (SI Figure S11). The stated uncertainty takes this assumption into account. The mass concentration of SOM produced from IEPOX isomers was estimated based on the decrease in gas-phase IEPOX concentration measured by SRI-NO^+-TOF-MS and corrected for the stoichiometric change in mass due to condensed-phase

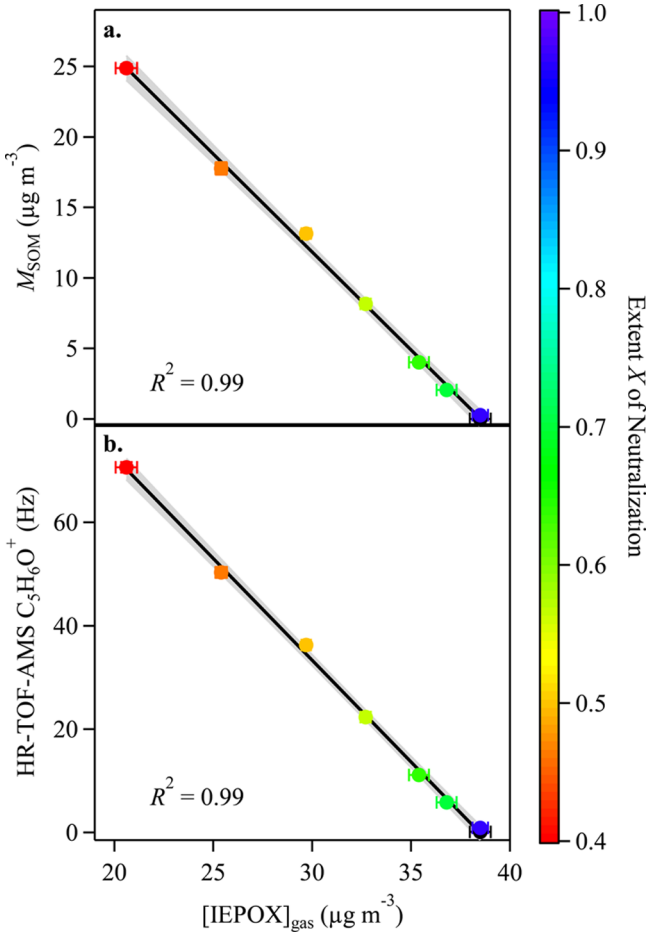

Figure 5. Correlation plot between the steady-state concentration $[IEPOX]_{gas}$ of IEPOX isomers in the gas phase measured by SRI-NO^+-TOF-MS and data sets recorded by HR-TOF-AMS of the outflow of Reactor 2. (a) Particle organic mass concentration, M_{SOM}. (b) AMS $C_5H_6O^+$ signal. The experiments are conducted using isoprene oxidation products produced in Reactor 1. Black lines show a linear fit of experimental data, and the gray region represents the 95% confidence interval of the fit. Data points are colored by the extent X of neutralization. The black data points represent experiments conducted when sulfate particles were not injected.

reactions, such as the addition of a water molecule (cf. SI). By this analysis, the decrease in gas-phase IEPOX mass concentration corresponded to (46 ± 11)% of the produced organic mass concentration (including wall-loss correction) across the experiments. The stated uncertainty includes a 5% uncertainty in the fitted slope of Figure 5a, a 20% uncertainty in the wall-loss correction for M_{SOM}, a 10% uncertainty in the sensitivity factor for gas-phase IEPOX detection, and an 8% uncertainty in the stoichiometric change of condensed-phase reactions of IEPOX compounds. Within the stated uncertainties, this result of an IEPOX contribution of (46 ± 11)% by consideration of gas-phase mass loss and particle-phase mass increment was consistent with the estimate of an IEPOX contribution of (59 ± 21)% (molecular counts) based on the total loss of gas-phase species. The two separate analyses lead to the common conclusion that the reactive uptake of IEPOX isomers accounted for half of the produced SOM, at least for isoprene photooxidation under HO_2-dominant conditions in the presence of acidic particles.

dx.doi.org/10.1021/es5034298 | *Environ. Sci. Technol.* 2015, 49, 250−258

The experiments also showed that the absolute loss of gas-phase IEPOX isomers and the associated production of SOM were greater for more acidic particles (i.e., lower X), even as the relative contribution of IEPOX to gas-phase loss and particle-phase production remained constant within the stated uncertainties. One possibility is that greater acidity promoted the reactive uptake of IEPOX isomers.[22,26,47] Another possibility is that for the conducted experiments the sulfate mass concentration, which has been suggested as a controlling factor of SOM production from the reactive uptake of epoxy compounds,[48] was higher for more acidic particles. Further experiments are needed to differentiate between these two possible explanations.

Figure 5b shows a scatter plot between the gas-phase concentration of IEPOX isomers and the corresponding intensity of the $C_5H_6O^+$ signal measured by the HR-TOF-AMS for the particle phase over a range of X. The decrease of the gas-phase IEPOX concentration and the increase of HR-TOF-AMS $C_5H_6O^+$ were correlated (R^2 = 0.99), suggesting that the HR-TOF-AMS $C_5H_6O^+$ signal of isoprene-derived SOM was directly related to the reactive uptake of IEPOX isomers. Given that the AMS uses electron-impact ionization, the AMS $C_5H_6O^+$ ion should not be interpreted as indicative of the direct presence of IEPOX isomers in the particle phase but rather of the possible presence of IEPOX isomers as well as their derivatives and other oxidation products having similar base structures that can all fragment to $C_5H_6O^+$. The correlation apparent in Figure 5b does, however, provide further positive support of the link between isoprene photooxidation products, in particular IEPOX isomers, and the HR-TOF-AMS $C_5H_6O^+$ signal (m/z 82). This signal has recently emerged in the literature as a suggested tracer fragment ion of isoprene-derived SOM in the atmosphere.[24,44−46]

The results presented thus far provide strong evidence from two different perspectives that the SOM production pathways tied to IEPOX isomers accounted for half of the SOM mass concentration for the investigated reaction conditions. The further open question is what the carbon sources of the other half of the produced SOM were. The signal decreases of the SRI-NO^+-TOF-MS mass spectra occurred across many ion peaks, in addition to that from $C_5H_6O^+$ ion (Figure 2). Due to fragmentation of oxygenated isoprene products (e.g., IEPOX isomers and ISOPOOH isomers)[29,49] and the existence of many isomers among known isoprene products, inference of the precursor compounds associated with the other ions (i.e., besides $C_5H_6O^+$) remains highly uncertain at the present time. A study using standard compounds is suggested for definitive insights.

Even though no definitive information regarding the carbon sources of isoprene SOM other than IEPOX isomers is presented, some speculative possibilities can still be considered. As one example, hydroxyl aldehydic epoxides ($C_5H_8O_3$) have recently been proposed as major oxidation products of IEPOX isomers in the gas phase.[27,50] These products might partition to the particle phase and undergo acid-catalyzed ring-opening reactions. The $C_5H_7O_2^+$ ion, which had the second largest decrease in gas-phase signal intensity in the present study, might arise from the reaction of the aldehydic epoxides ($C_5H_8O_3$) with NO^+ by OH^- transfer.[40] Another possible contributing process might be the thermodynamically driven partitioning of semivolatile organic products into the IEPOX-derived SOM. This hypothesis is consistent with the observation that the signal decreased across many peaks in Figure 2a as well as the approximate independence of the fraction of IEPOX-derived SOM for different values of X (Table 1).

Atmospheric Implications. The simultaneous monitoring of the loss of gas-phase species and the production of particle-phase mass establishes that the uptake of IEPOX isomers explains (46 ± 11)% of the SOM mass concentration produced from isoprene photooxidation for HO_2-dominant conditions in the presence of acidic particles at low relative humidity. Atmospheric chemistry models have recently begun to incorporate isoprene-derived SOM production via reactive uptake, with a focus on IEPOX isomers.[10,51] An uncertainty, however, in the validity of these treatments has been the importance of IEPOX relative to other products of isoprene photooxidation for SOM production. The results of the present study provide a direct experimental basis to support the appropriateness of these recent additions to models by finding that IEPOX isomers account for half of SOM produced under laboratory conditions and demonstrating that SOM production in the particle phase is proportional to IEPOX loss from the gas phase.

Although the present study explored a range of particle acidity, the experiments were conducted only for low relative humidity (<5%). The result is a relatively low particle water content. For instance, pure sulfuric acid at 10% RH and 20 °C has half as much absorbed water as at 50% RH.[52] The implication is that acid-catalyzed reactions might be faster at <5% RH compared to elevated RH. Another possibility, however, is that other competing mechanisms, which are less important at elevated RH, can become kinetically favorable at the higher ionic strength of the lower RH. Given the close connections between IEPOX reactivity and acidity on the one hand and acidity and water content on the other hand, further laboratory studies are warranted across the range of atmospheric humidities.

■ ASSOCIATED CONTENT

Ⓢ Supporting Information

Experimental methods and additional figures. This material is available free of charge via the Internet at http://pubs.acs.org.

■ AUTHOR INFORMATION

Corresponding Authors

*Phone: 617-495-2858; e-mail: kamckinney@seas.harvard.edu.
*Phone: 617-495-7620; fax: 617-496-1471; e-mail: scot_martin@harvard.edu.

Present Address

[⊥]Now at Division of Earth Sciences, Nanyang Technological University, Singapore, and Earth Observatory of Singapore

Author Contributions

[∥]These authors contributed equally to this paper

Notes

The authors declare no competing financial interest.

■ ACKNOWLEDGMENTS

Support was received from the U.S. National Science Foundation (Grant No. ATM-0959452 and CHE-1212692), the U.S. Department of Energy (Grant No. DE-FG02-08ER64529), and the Institute for Sustainability and Energy at Northwestern (ISEN). Y.J. Liu acknowledges a NASA Earth and Space Science Fellowship. We acknowledge Q. Chen, N. H. Robinson, H. Coe, S.H. Budisulistiorini, J. D. Surratt, J. G.

Slowik, and J. P. D. Abbatt for making available PMF results from their studies and helpful discussion.

REFERENCES

(1) Pope, C. A., III; Dockery, D. W. Health effects of fine particulate air pollution: Lines that connect. *J. Air Waste Manage. Assoc.* **2006**, *56* (6), 709−742.

(2) Charlson, R. J. Atmospheric visibility related to aerosol mass concentration: Review. *Environ. Sci. Technol.* **1969**, *3* (10), 913−918.

(3) Jacob, D. *Introduction to Atmospheric Chemistry*. Princeton University Press, 1999; p 148−152.

(4) Zhang, Q.; Jimenez, J. L.; Canagaratna, M. R.; Allan, J. D.; Coe, H.; Ulbrich, I.; Alfarra, M. R.; Takami, A.; Middlebrook, A. M.; Sun, Y. L.; Dzepina, K.; Dunlea, E.; Docherty, K.; DeCarlo, P. F.; Salcedo, D.; Onasch, T.; Jayne, J. T.; Miyoshi, T.; Shimono, A.; Hatakeyama, S.; Takegawa, N.; Kondo, Y.; Schneider, J.; Drewnick, F.; Borrmann, S.; Weimer, S.; Demerjian, K.; Williams, P.; Bower, K.; Bahreini, R.; Cottrell, L.; Griffin, R. J.; Rautiainen, J.; Sun, J. Y.; Zhang, Y. M.; Worsnop, D. R. Ubiquity and dominance of oxygenated species in organic aerosols in anthropogenically-influenced Northern Hemisphere midlatitudes. *Geophys. Res. Lett.* **2007**, *34* (13), L13801.

(5) Hallquist, M.; Wenger, J. C.; Baltensperger, U.; Rudich, Y.; Simpson, D.; Claeys, M.; Dommen, J.; Donahue, N. M.; George, C.; Goldstein, A. H.; Hamilton, J. F.; Herrmann, H.; Hoffmann, T.; Iinuma, Y.; Jang, M.; Jenkin, M. E.; Jimenez, J. L.; Kiendler-Scharr, A.; Maenhaut, W.; McFiggans, G.; Mentel, T. F.; Monod, A.; Prevot, A. S. H.; Seinfeld, J. H.; Surratt, J. D.; Szmigielski, R.; Wildt, J. The formation, properties and impact of secondary organic aerosol: Current and emerging issues. *Atmos. Chem. Phys.* **2009**, *9* (14), 5155−5236.

(6) Kroll, J. H.; Seinfeld, J. H. Chemistry of secondary organic aerosol: Formation and evolution of low-volatility organics in the atmosphere. *Atmos. Environ.* **2008**, *42* (16), 3593−3624.

(7) Henze, D. K.; Seinfeld, J. H. Global secondary organic aerosol from isoprene oxidation. *Geophys. Res. Lett.* **2006**, *33* (9), L09812.

(8) Hoyle, C. R.; Berntsen, T.; Myhre, G.; Isaksen, I. S. A. Secondary organic aerosol in the global aerosol—Chemical transport model Oslo CTM2. *Atmos. Chem. Phys.* **2007**, *7* (21), 5675−5694.

(9) Heald, C. L.; Henze, D. K.; Horowitz, L. W.; Feddema, J.; Lamarque, J. F.; Guenther, A.; Hess, P. G.; Vitt, F.; Seinfeld, J. H.; Goldstein, A. H.; Fung, I. Predicted change in global secondary organic aerosol concentrations in response to future climate, emissions, and land use change. *J. Geophys. Res.* **2008**, *113* (D5), D05211.

(10) Lin, G.; Penner, J. E.; Sillman, S.; Taraborrelli, D.; Lelieveld, J. Global modeling of SOA formation from dicarbonyls, epoxides, organic nitrates and peroxides. *Atmos. Chem. Phys.* **2012**, *12* (10), 4743−4774.

(11) Guenther, A.; Karl, T.; Harley, P.; Wiedinmyer, C.; Palmer, P. I.; Geron, C. Estimates of global terrestrial isoprene emissions using MEGAN (model of emissions of gases and aerosols from nature). *Atmos. Chem. Phys.* **2006**, *6* (11), 3181−3210.

(12) Archibald, A. T.; Cooke, M. C.; Utembe, S. R.; Shallcross, D. E.; Derwent, R. G.; Jenkin, M. E. Impacts of mechanistic changes on HO_x formation and recycling in the oxidation of isoprene. *Atmos. Chem. Phys.* **2010**, *10* (17), 8097−8118.

(13) Claeys, M.; Graham, B.; Vas, G.; Wang, W.; Vermeylen, R.; Pashynska, V.; Cafmeyer, J.; Guyon, P.; Andreae, M. O.; Artaxo, P.; Maenhaut, W. Formation of secondary organic aerosols through photooxidation of isoprene. *Science* **2004**, *303* (5661), 1173−1176.

(14) Wang, W.; Kourtchev, I.; Graham, B.; Cafmeyer, J.; Maenhaut, W.; Claeys, M. Characterization of oxygenated derivatives of isoprene related to 2-methyltetrols in Amazonian aerosols using trimethylsilylation and gas chromatography/ion trap mass spectrometry. *Rapid Commun. Mass Spectrom.* **2005**, *19* (10), 1343−1351.

(15) Surratt, J. D.; Murphy, S. M.; Kroll, J. H.; Ng, N. L.; Hildebrandt, L.; Sorooshian, A.; Szmigielski, R.; Vermeylen, R.; Maenhaut, W.; Claeys, M.; Flagan, R. C.; Seinfeld, J. H. Chemical composition of secondary organic aerosol formed from the photooxidation of isoprene. *J. Phys. Chem. A* **2006**, *110* (31), 9665−9690.

(16) Surratt, J. D.; Kroll, J. H.; Kleindienst, T. E.; Edney, E. O.; Claeys, M.; Sorooshian, A.; Ng, N. L.; Offenberg, J. H.; Lewandowski, M.; Jaoui, M.; Flagan, R. C.; Seinfeld, J. H. Evidence for organosulfates in secondary organic aerosol. *Environ. Sci. Technol.* **2007**, *41* (2), 517−527.

(17) Chan, M. N.; Surratt, J. D.; Claeys, M.; Edgerton, E. S.; Tanner, R. L.; Shaw, S. L.; Zheng, M.; Knipping, E. M.; Eddingsaas, N. C.; Wennberg, P. O.; Seinfeld, J. H. Characterization and quantification of isoprene-derived epoxydiols in ambient aerosol in the southeastern United States. *Environ. Sci. Technol.* **2010**, *44* (12), 4590−4596.

(18) Froyd, K. D.; Murphy, S. M.; Murphy, D. M.; de Gouw, J. A.; Eddingsaas, N. C.; Wennberg, P. O. Contribution of isoprene-derived organosulfates to free tropospheric aerosol mass. *Proc. Natl. Acad. Sci. U.S.A.* **2010**, *107* (50), 21360−21365.

(19) Carlton, A. G.; Wiedinmyer, C.; Kroll, J. H. A review of secondary organic aerosol (SOA) formation from isoprene. *Atmos. Chem. Phys.* **2009**, *9* (14), 4987−5005.

(20) Paulot, F.; Crounse, J. D.; Kjaergaard, H. G.; Kurten, A., St; Clair, J. M.; Seinfeld, J. H.; Wennberg, P. O. Unexpected epoxide formation in the gas-phase photooxidation of isoprene. *Science* **2009**, *325* (5941), 730−733.

(21) Surratt, J. D.; Chan, A. W. H.; Eddingsaas, N. C.; Chan, M. N.; Loza, C. L.; Kwan, A. J.; Hersey, S. P.; Flagan, R. C.; Wennberg, P. O.; Seinfeld, J. H. Reactive intermediates revealed in secondary organic aerosol formation from isoprene. *Proc. Natl. Acad. Sci. U.S.A.* **2010**, *107* (15), 6640−6645.

(22) Cole-Filipiak, N. C.; O'Connor, A. E.; Elrod, M. J. Kinetics of the hydrolysis of atmospherically relevant isoprene-derived hydroxy epoxides. *Environ. Sci. Technol.* **2010**, *44* (17), 6718−6723.

(23) Lin, Y. H.; Zhang, Z.; Docherty, K. S.; Zhang, H.; Budisulistiorini, S. H.; Rubitschun, C. L.; Shaw, S. L.; Knipping, E. M.; Edgerton, E. S.; Kleindienst, T. E.; Gold, A.; Surratt, J. D. Isoprene epoxydiols as precursors to secondary organic aerosol formation: Acid-catalyzed reactive uptake studies with authentic compounds. *Environ. Sci. Technol.* **2011**, *46* (1), 250−258.

(24) Budisulistiorini, S. H.; Canagaratna, M. R.; Croteau, P. L.; Marth, W. J.; Baumann, K.; Edgerton, E. S.; Shaw, S. L.; Knipping, E. M.; Worsnop, D. R.; Jayne, J. T.; Gold, A.; Surratt, J. D. Real-time continuous characterization of secondary organic aerosol derived from Isoprene epoxydiols in downtown Atlanta, Georgia, using the Aerodyne aerosol chemical speciation monitor. *Environ. Sci. Technol.* **2013**, *47* (11), 5686−5694.

(25) Nguyen, T. B.; Coggon, M. M.; Bates, K. H.; Zhang, X.; Schwantes, R. H.; Schilling, K. A.; Loza, C. L.; Flagan, R. C.; Wennberg, P. O.; Seinfeld, J. H. Organic aerosol formation from the reactive uptake of isoprene epoxydiols (IEPOX) onto non-acidified inorganic seeds. *Atmos. Chem. Phys.* **2014**, *14* (7), 3497−3510.

(26) Gaston, C. J.; Riedel, T. P.; Zhang, Z.; Gold, A.; Surratt, J. D.; Thornton, J. A. Reactive uptake of an isoprene-derived epoxydiol to submicron aerosol particles. *Environ. Sci. Technol.* **2014**, *48* (19), 11178−11186.

(27) Bates, K. H.; Crounse, J. D.; St. Clair, J. M.; Bennett, N. B.; Nguyen, T. B.; Seinfeld, J. H.; Stoltz, B. M.; Wennberg, P. O. Gas phase production and loss of isoprene epoxydiols. *J. Phys. Chem. A* **2014**, *118* (7), 1237−1246.

(28) Chen, Q.; Liu, Y. J.; Donahue, N. M.; Shilling, J. E.; Martin, S. T. Particle-phase chemistry of secondary organic material: Modeled compared to measured O:C and H:C elemental ratios provide constraints. *Environ. Sci. Technol.* **2011**, *45* (11), 4763−4770.

(29) Liu, Y. J.; Herdlinger-Blatt, I.; McKinney, K. A.; Martin, S. T. Production of methyl vinyl ketone and methacrolein via the hydroperoxyl pathway of isoprene oxidation. *Atmos. Chem. Phys.* **2013**, *13* (11), 5715−5730.

(30) Lelieveld, J.; Butler, T. M.; Crowley, J. N.; Dillon, T. J.; Fischer, H.; Ganzeveld, L.; Harder, H.; Lawrence, M. G.; Martinez, M.; Taraborrelli, D.; Williams, J. Atmospheric oxidation capacity sustained by a tropical forest. *Nature* **2008**, *452* (7188), 737−740.

(31) Crounse, J. D.; Paulot, F.; Kjaergaard, H. G.; Wennberg, P. O. Peroxy radical isomerization in the oxidation of isoprene. *Phys. Chem. Chem. Phys.* **2011**, *13* (30), 13607−13613.
(32) Xie, Y.; Paulot, F.; Carter, W. P. L.; Nolte, C. G.; Luecken, D. J.; Hutzell, W. T.; Wennberg, P. O.; Cohen, R. C.; Pinder, R. W. Understanding the impact of recent advances in isoprene photooxidation on simulations of regional air quality. *Atmos. Chem. Phys.* **2013**, *13* (16), 8439−8455.
(33) Jang, M.; Czoschke, N. M.; Lee, S.; Kamens, R. M. Heterogeneous atmospheric aerosol production by acid-catalyzed particle-phase reactions. *Science* **2002**, *298* (5594), 814−817.
(34) Surratt, J. D.; Lewandowski, M.; Offenberg, J. H.; Jaoui, M.; Kleindienst, T. E.; Edney, E. O.; Seinfeld, J. H. Effect of acidity on secondary organic aerosol formation from isoprene. *Environ. Sci. Technol.* **2007**, *41* (15), 5363−5369.
(35) Kuwata, M.; Liu, Y. J.; McKinney, K. A.; Martin, S. T. Phase of inorganic sulfate can regulate the production of secondary organic material from isoprene photooxidation products *Phys. Chem. Chem. Phys.*, submitted.
(36) Kuwata, M.; Martin, S. T. Phase of atmospheric secondary organic material affects its reactivity. *Proc. Natl. Acad. Sci. U.S.A.* **2012**, *109* (43), 17354−17359.
(37) Jordan, A.; Haidacher, S.; Hanel, G.; Hartungen, E.; Märk, L.; Seehauser, H.; Schottkowsky, R.; Sulzer, P.; Märk, T. D. A high resolution and high sensitivity proton-transfer-reaction time-of-flight mass spectrometer (PTR-TOF-MS). *Int. J. Mass. Spectrom.* **2009**, *286* (2−3), 122−128.
(38) Jordan, A.; Haidacher, S.; Hanel, G.; Hartungen, E.; Herbig, J.; Märk, L.; Schottkowsky, R.; Seehauser, H.; Sulzer, P.; Märk, T. D. An online ultra-high sensitivity proton-transfer-reaction mass-spectrometer combined with switchable reagent ion capability (PTR+SRI-MS). *Int. J. Mass. Spectrom.* **2009**, *286* (1), 32−38.
(39) DeCarlo, P. F.; Kimmel, J. R.; Trimborn, A.; Northway, M. J.; Jayne, J. T.; Aiken, A. C.; Gonin, M.; Fuhrer, K.; Horvath, T.; Docherty, K. S.; Worsnop, D. R.; Jimenez, J. L. Field-deployable, high-resolution, time-of-flight aerosol mass spectrometer. *Anal. Chem.* **2006**, *78* (24), 8281−8289.
(40) Smith, D.; Spanel, P. Selected Ion Flow Tube Mass Spectrometry (SIFT-MS) for on-line trace gas analysis. *Mass. Spectrom. Rev.* **2005**, *24* (5), 661−700.
(41) Taipale, R.; Ruuskanen, T. M.; Rinne, J.; Kajos, M. K.; Hakola, H.; Pohja, T.; Kulmala, M. Technical note: Quantitative long-term measurements of VOC concentrations by PTR-MS—Measurement, calibration, and volume mixing ratio calculation methods. *Atmos. Chem. Phys.* **2008**, *8* (22), 6681−6698.
(42) Ebben, C. J.; Strick, B. F.; Upshur, M. A.; Chase, H. M.; Achtyl, J. L.; Thomson, R. J.; Geiger, F. M. Towards the identification of molecular constituents associated with the surfaces of isoprene-derived secondary organic aerosol (SOA) particles. *Atmos. Chem. Phys.* **2014**, *14* (5), 2303−2314.
(43) Pankow, J. F.; Asher, W. E. SIMPOL.1: A simple group contribution method for predicting vapor pressures and enthalpies of vaporization of multifunctional organic compounds. *Atmos. Chem. Phys.* **2008**, *8* (10), 2773−2796.
(44) Robinson, N. H.; Hamilton, J. F.; Allan, J. D.; Langford, B.; Oram, D. E.; Chen, Q.; Docherty, K.; Farmer, D. K.; Jimenez, J. L.; Ward, M. W.; Hewitt, C. N.; Barley, M. H.; Jenkin, M. E.; Rickard, A. R.; Martin, S. T.; McFiggans, G.; Coe, H. Evidence for a significant proportion of secondary organic aerosol from isoprene above a maritime tropical forest. *Atmos. Chem. Phys.* **2011**, *11* (3), 1039−1050.
(45) Slowik, J. G.; Brook, J.; Chang, R. Y. W.; Evans, G. J.; Hayden, K.; Jeong, C. H.; Li, S. M.; Liggio, J.; Liu, P. S. K.; McGuire, M.; Mihele, C.; Sjostedt, S.; Vlasenko, A.; Abbatt, J. P. D. Photochemical processing of organic aerosol at nearby continental sites: Contrast between urban plumes and regional aerosol. *Atmos. Chem. Phys.* **2011**, *11* (6), 2991−3006.
(46) Chen, Q.; Farmer, D. K.; Rizzo, L. V.; Pauliquevis, T.; Kuwata, M.; Karl, T. G.; Guenther, A.; Allan, J. D.; Coe, H.; Andreae, M. O.; Pöschl, U.; Jimenez, J. L.; Artaxo, P.; Martin, S. T. Fine-mode organic mass concentrations and sources in the Amazonian wet season (AMAZE-08). *Atmos. Chem. Phys. Discuss.* **2014**, *14* (11), 16151−16186.
(47) Eddingsaas, N. C.; VanderVelde, D. G.; Wennberg, P. O. Kinetics and products of the acid-catalyzed ring-opening of atmospherically relevant butyl epoxy alcohols. *J. Phys. Chem. A* **2010**, *114* (31), 8106−8113.
(48) Iinuma, Y.; Boge, O.; Kahnt, A.; Herrmann, H. Laboratory chamber studies on the formation of organosulfates from reactive uptake of monoterpene oxides. *Phys. Chem. Chem. Phys.* **2009**, *11* (36), 7985−7997.
(49) Nguyen, T. B.; Crounse, J. D.; Schwantes, R. H.; Teng, A. P.; Bates, K. H.; Zhang, X.; St. Clair, J. M.; Brune, W. H.; Tyndall, G. S.; Keutsch, F. N.; Seinfeld, J. H.; Wennberg, P. O. Overview of the Focused Isoprene eXperiments at California Institute of Technology (FIXCIT): Mechanistic chamber studies on the oxidation of biogenic compounds. *Atmos. Chem. Phys. Discuss.* **2014**, *14* (15), 21611−21658.
(50) Jacobs, M. I.; Darer, A. I.; Elrod, M. J. Rate constants and products of the OH reaction with isoprene-derived epoxides. *Environ. Sci. Technol.* **2013**, *47*, 12866−12876.
(51) Pye, H. O. T.; Pinder, R. W.; Piletic, I. R.; Xie, Y.; Capps, S. L.; Lin, Y.-H.; Surratt, J. D.; Zhang, Z.; Gold, A.; Luecken, D. J.; Hutzell, W. T.; Jaoui, M.; Offenberg, J. H.; Kleindienst, T. E.; Lewandowski, M.; Edney, E. O. Epoxide pathways improve model predictions of isoprene markers and reveal key role of acidity in aerosol formation. *Environ. Sci. Technol.* **2013**, *47* (19), 11056−11064.
(52) Wexler, A. S.; Clegg, S. L. Atmospheric aerosol models for systems including the ions H^+, NH_4^+, Na^+, SO_4^{2-}, NO_3^-, Cl^-, Br^-, and H_2O. *J. Geophys. Res.* **2002**, *107* (D14), 4207.
(53) Mifflin, A. L.; Smith, M. L.; Martin, S. T. Morphology hypothesized to influence aerosol particle deliquescence. *Phys. Chem. Chem. Phys.* **2009**, *11* (43), 10095−107.
(54) Schlenker, J. C.; Martin, S. T. Crystallization pathways of sulfate-nitrate-ammonium aerosol particles. *J. Phys. Chem. A* **2005**, *109* (44), 9980−5.